A supramolecular chemistry approach for potentiating live attenuated whole-organism vaccines

Duszenko, N.

4

Chemically enhanced immunogenicity of bacteria by supramolecular functionalization with an adjuvant

Nikolas Duszenko, Danny M. van Willigen, Anton Bunschoten, Aldrik H. Velders, Meta Roestenberg and Fijs W.B. van Leeuwen

Adapted from:

Chembiochem. 2022 Sep 30;e202200434.
PMID: 36177993
DOI: 10.1002/cbic.202200434.

Abstract

Many pathogens blunt immune responses by lacking immunogenic structural features, which typically results in disease. Here, we show evidence suggesting that pathogen immunogenicity can be chemically enhanced. Using supramolecular host-guest chemistry, we complexed onto the surface of a poorly immunogenic bacterium (*Staphylococcus aureus*) a TLR7 agonist-based adjuvant. "Adjuvanted" bacteria were still readily recognized by macrophages and induced a more pro-inflammatory immunophenotype. Future applications of this concept could yield treatment modalities that bolster the immune system's response to pathogenic microbes.

Introduction

Immune responses to pathogens are critically dependent on recognition of pathogen-associated molecular patterns (PAMPs) (Medzhitov, 2007). Sentinel immune cells such as macrophages possess a suite of receptors facilitating recognition, such as Toll-like receptors (TLRs), activation of which triggers the development of an antimicrobial phenotype characterized by e.g. increased secretion of pro-inflammatory cytokines (Sica et al., 2015). Accordingly, many pathogens have evolved mechanisms for avoiding such activation (Ballou et al., 2016; Cambier et al., 2014; Gault et al., 2015). For example, the bacterium Staphylococcus aureus enzymatically cleaves some of its surface components and renders them inert to immune cells, endowing it with a low immunogenicity that yields suboptimal immune activation and can lead to chronic metastatic infection and disease (Chen and Alonzo, 2019).

The issue of low immunogenicity has long been known in vaccinology and led to the concept of adjuvanting: addition of exogenous immunogens called "adjuvants" to boost entities' immunogenicity (Di Pasquale et al., 2015). Clinically registered subunit vaccines such as Prevnar and RTS,S (Cadoz, 1998; Rutgers et al., 1988), as well as next-generation nanoparticle vaccines (Francica et al., 2016; Wilson et al., 2013), have shown that tightly tethering immunogens tends to yield better boosts in immunogenicity. We thus reasoned that the same concept might be translated to improve (pathogenic) microbes' immunogenicity.

Here, we show the conceptual feasibility of boosting the immunogenicity of S. aureus bacteria by chemically modifying the cell surface with the synthetic TLR7 agonist-based adjuvant CL307. This adjuvant was chosen due to a number of useful properties: 1) a reactive spermine moiety for conjugating to host polymers that would facilitate recognition of the agonist by TLR7; 2) a small size (597 Da) with minimal impact on the host polymers' chemical properties; and 3) an absorption at 298 nm that allowed for quantitation. The resulting "adjuvanted" bacteria were normally recognized by macrophages and yielded improved immune activation compared to unadulterated bacteria.

Results and Discussion

To introduce CL307 onto the surface of S. aureus bacteria, we adapted a supramolecular host-guest chemistry technique for functionalizing the cell surface of live bacterial and eukaryotic cells (Figure 1) (Duszenko et al., 2020a; Rood et al., 2017). An initial pre-functionalization of the surface with an adamantane (Ad) moiety was achieved via a bacteria-targeting Ad-UBI29-41 construct, as the UBI29-41 vector constitutes a cationic, antimicrobial peptide that inserts into the bacterial cell membrane (Welling et al., 2000). This Ad pre-functionalization was followed by the complexation of complementary β-cyclodextrin (CD)-bearing PIBMA polymers that can, in addition to CD, serve as carrier for other functionalities of interest. Here, these functionalities comprised 1) Cy5 dyes for tracking the polymers, and 2) the adjuvant CL307.

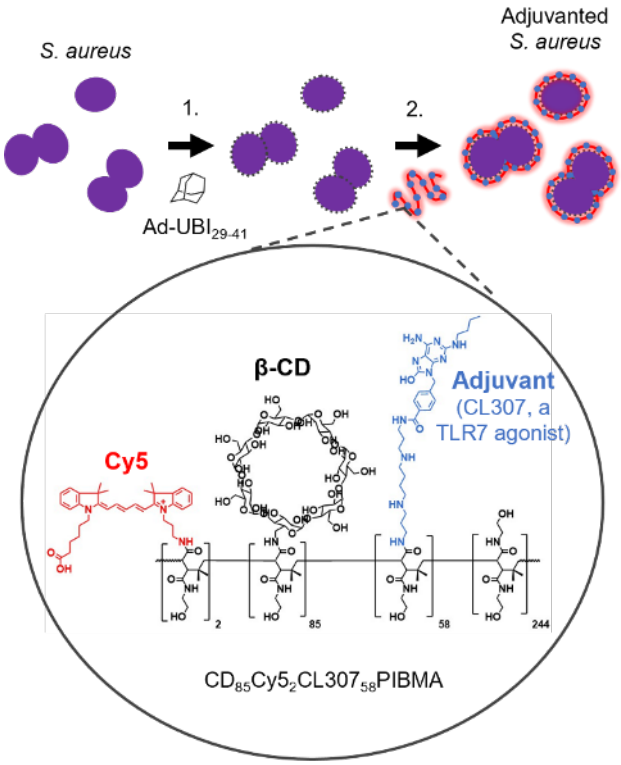

Figure 1: Schematic illustrating chemical strategy for introducing an adjuvant onto the surface of S. aureus bacteria. The bacterial surface was first pre-functionalized with Ad using the antibacterial peptide UBI29-41 as a vector, followed by supramolecular complexation of CD- and CL307-bearing polymers onto the cell surface. Ad = adamantane; UBI = ubiquicidin; CD = β-cyclodextrin.

Despite the presence of approximately 57 units of CL307 per host polymer (Supplemental Figure 2), the polymers could still complex well to the Ad-pre-functionalized S. aureus surface. Confocal imaging showed virtually all bacteria with strong Cy5 signals indicative of complexed polymer on the bacterial cell surface, signals adjacent to Hoechst counterstaining of the cytoplasm (Figure 2a). ImageJ analysis of an adjuvanted bacterium's cross section validated these findings, with distinct Cy5 signals flanking the Hoechst signal of the bacterium's cytoplasm (Figure 2b).

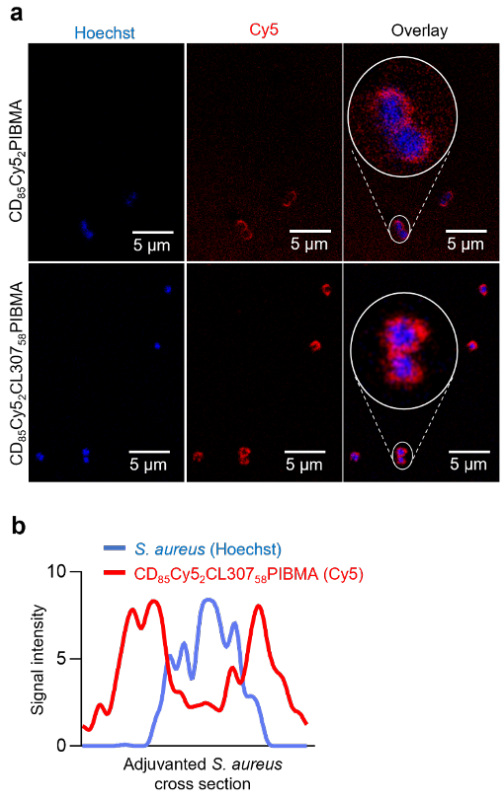

Figure 2: Complexation of CL307-bearing host polymers onto the bacterial cell surface to yield adjuvanted S. aureus. a) Confocal fluorescence microscopy images of bacteria with complexed host polymer (top row) and CL307-bearing host polymer (bottom row) showing Hoechst signal from the bacterial cytoplasm (left – blue), Cy5 signal from complexed (CL307-bearing) polymers on the bacterial cell surface (middle – red), and an overlay of the two signals (right). b) ImageJ analysis quantitating Hoechst and Cy5 signal intensities in a cross section of one adjuvanted bacterium.

Flow cytometric analysis was subsequently used to gauge the efficiency of generating adjuvanted S. aureus. The supramolecular system employed was found to be highly efficient, with virtually all bacteria showing varying quantities of CL307-bearing polymer complexed (Figure 3a; median Cy5 signal of 8,610±1,914 A.U. (i) vs. 0.9±0.7 A.U. (iv)). Notably, CL307-bearing polymers were much less effectively complexed to bacteria without Ad-pre-functionalization (Figure 3a, panel ii – 7-fold less). To estimate the average quantity of CL307 per bacterium, median Cy5 signal was converted into absolute equivalents Cy5 dye via commercial fluorescence quantification beads (Figure 3b). This conversion yielded an average of 105 polymers per bacterium, indicating the presence of about 107 units of CL307 per bacterium – a quantity on the same order of magnitude as seen in adjuvanted nanoparticle vaccines (Francica et al., 2016; Wilson et al., 2013).

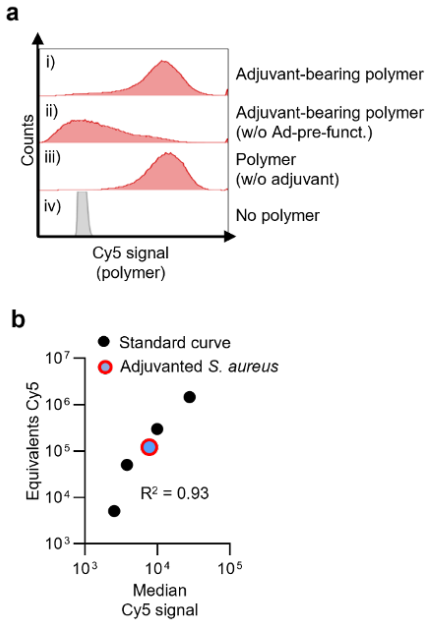

Figure 3: Quantitative flow cytometric analysis of adjuvanted S. aureus. a) Representative flow cytometry histogram of Cy5 signals (x-axis, log scale) in a sample of S. aureus complexed with CL307-bearing polymer (i), S. aureus complexed with little CL307-bearing polymer in the absence of Ad-pre-functionalization (ii), S. aureus complexed with polymer lacking CL307 (iii) and control S. aureus (iv). b) Plot of adjuvanted S. aureus' median Cy5 signal (red-blue) in relation to fluorescence quantification beads (black) of varying Cy5 intensities.

Flow cytometric analysis was further used to characterize the supramolecular chemical system when adapted for introducing adjuvants onto the S. aureus cell surface. The presence of about 57 CL307 units per polymer did not preclude complexation at levels comparable to parental polymer analog lacking CL307 (Figure 4a; 8,610±1,914 vs. 9,342±1,171 A.U., $p = 0.6020$). Remarkably, optimal complexation was however dependent on a slightly elevated salinity during complexation (Supplemental Figure 6), an effect that has previously been described for enhancing supramolecular host-guest interactions (Buvari and Barcza, 1979; Mochida et al., 1973). Supramolecular host-guest interactions were critical for maximizing polymer complexation: the absence of Ad-pre-functionalization decreased complexation 7-fold (Figure 4a; 1,130±122 vs. 8,610±1,914, $p < 0.01$), and competition experiments using an excess of 1 mM soluble Ad similarly decreased complexation (Figure 4b; 1,774±74 vs. 11,574±991 A.U., $p < 0.0001$). Once formed, adjuvanted S. aureus remained stably associated, with over 95% of CL307-bearing polymers remaining complexed after 24 hours incubation at physiological conditions (Figure 4c; 48,593±2,652 A.U. at t = 24h vs. 49,736±1,564 A.U. at t = 0). In line with previous work (Duszenko et al., 2020a; Rood et al., 2017), complexed CL307-bearing polymers did not adversely affect bacterial viability, with comparable culture growth relative to control bacteria (Figure 4d; 0.492±0.005 vs. 0.486±0.012 A.U., $p = 0.481$).

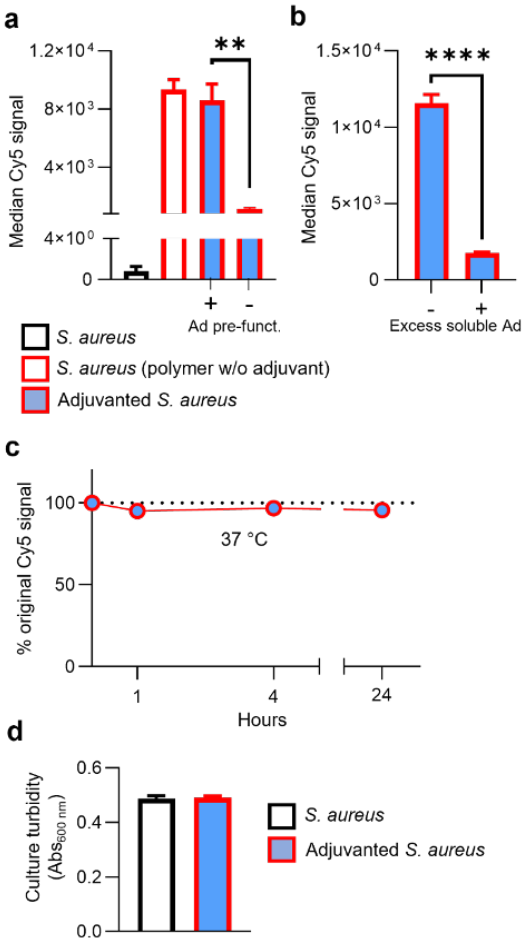

Figure 4: (Bio)chemical characteristics of supramolecular system underlying adjuvanted S. aureus. a) Median Cy5 signal (y-axis) of flow cytometric analysis of S. aureus controls (black), S. aureus with non-adjuvant polymer complexed (red), and adjuvanted S. aureus (red-blue) in the presence (+) and absence (-) of Ad-pre-functionalization (x-axis). b) Median Cy5 signal (y-axis) of flow cytometry-based competition experiment of adjuvanted S. aureus generated in the absence and presence (x-axis) of excess (1 mM) soluble Ad. c) Percent remaining median Cy5 signal (y-axis) of adjuvanted S. aureus after 24 hours incubation (x-axis) in PBS. d) Culture turbidity measurements by absorbance (y-axis) of adjuvanted S. aureus (red-blue) and control S. aureus (black) (x-axis) after 16 hours incubation at 37 °C in growth media. All data shown are from representative experiments of n = 3. Ad = adamantane; ** = $p < 0.01$, **** = $p < 0.0001$.

To investigate the immunological characteristics of adjuvanted S. aureus, a monocyte-derived macrophage assay was used as previously described (Duszenko et al., 2020a), as macrophages are reported to be key players in an effective immune responses to this pathogen (Flannagan et al., 2015; Pidwill et al., 2020). Confocal imaging showed that the presence of synthetic adjuvants on the S. aureus surface did not prevent macrophages from normally phagocytosing such bacteria (Figure 5) – all adjuvanted S. aureus were phagocytosed within 20 minutes.

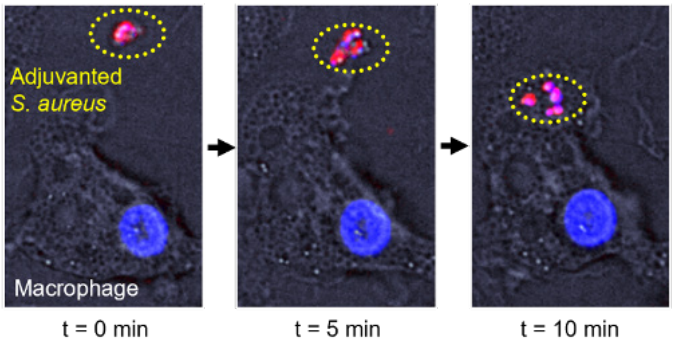

Figure 5: Phagocytosis of adjuvanted S. aureus by a monocyte-derived macrophage. Time-lapse confocal fluorescence microscopy images at t = 0 (left), t = 5 minutes (middle) and t = 10 minutes (right) of a macrophage (cell nucleus in blue) encountering and phagocytosing adjuvanted S. aureus (yellow dotted oval).

Finally, the immunogenicity of adjuvanted S. aureus relative to control S. aureus was assayed by measuring macrophage cytokine secretion during 24 hours of bacterial exposure. Adjuvanted S. aureus induced significantly increased secretion of pro-inflammatory IL-6 (Figure 6a), with 4-fold increases compared to both control S. aureus (1,686±238 vs. 480±193 pg/mL, $p < 0.01$) and S. aureus bearing polymer without CL307 (1,686±238 vs. 479±55 pg/mL, $p < 0.01$). CL307 conjugated to the S. aureus surface also induced a trend towards a higher IL-6 secretion compared to a mixture of S. aureus and soluble concentration-matched CL307 (1,686±238 vs. 940±322 pg/mL, $p = 0.1169$). Secretion of anti-inflammatory IL-10 was on the other hand less changed by adjuvanted S. aureus (Figure 6b). IL-10 secretion to adjuvanted S. aureus was comparable to both control S. aureus (117±37 vs. 67±13 pg/mL, $p = 0.6408$) and S. aureus bearing polymer without CL307 (117±37 vs. 60±6 pg/mL, $p = 0.5370$). Notably, IL-10 secretion in response to adjuvanted S. aureus was however significantly lower compared to S. aureus + CL307 mixture (117±37 vs. 261±45 pg/mL, $p < 0.05$).

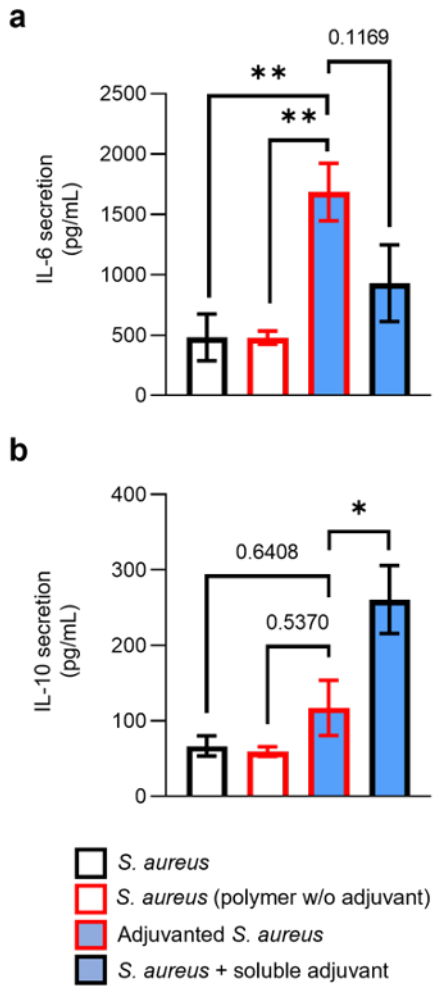

Figure 6: Cytokine secretion by monocyte-derived macrophages after 24 hours of exposure to adjuvanted S. aureus and controls. a) IL-6 secretion (y-axis, pg/mL) in response to S. aureus controls (black), S. aureus bearing polymer without CL307 (red), adjuvanted S. aureus (red-blue), and a mixture of S. aureus and soluble concentration-matched CL307 (black-blue) (x-axis). b) IL-10 secretion (y-axis, pg/mL) in response to S. aureus controls (black), S. aureus bearing polymer without CL307(red), adjuvanted S. aureus (red-blue), and a mixture of S. aureus and soluble concentration-matched CL307 (black-blue) (x-axis). Data shown are n = 5 from 2 independent experiments. IL-6 = interleukin-6; IL-10 = interleukin-10; * = $p < 0.05$, ** = $p < 0.01$.

Altogether, these results indicated that macrophages responded with a slightly more pro-inflammatory IL-6 response to S. aureus whose cell surface was chemically modified with CL307 – an effect that was positively impacted by physically connecting CL307 to the bacteria. Production of pro- and anti-inflammatory mediators such as IL-6 and IL-10, respectively, are constantly balanced to properly calibrate immune responses between too much and too little activation; usually, when one goes up, so does the other. The reversed trends in cytokine production patterns of IL-6 and IL-10 observed for the conjugated and soluble compound (Figure 6) exemplify a shift in that balance. Whereas soluble presentation of CL307 induced a mixed pro- and anti-inflammatory response in macrophages, conjugated CL307 induced a predominantly pro-inflammatory response. Future studies will need to determine if similar shifts towards a more pro-inflammatory response also apply to other immune cell models. Additionally, in vivo models will need to be used to gauge the potential (clinical) utility of the shifts here observed in vitro.

The findings here described suggest that chemical augmentation of microbial cell surfaces with adjuvants may indeed offer a strategy for improving such microbes' immunogenicity. In the future, UBI29-41 vectors' ability to "tag" offending bacteria in vivo (Chen et al., 2015; Ebenhan et al., 2014; Huang et al., 2017; Welling et al., 2019a; Zavadovskaya et al., 2021) could provide a basis to exploit supramolecular pre-targeting strategies (Spa et al., 2018; Welling et al., 2021; Welling et al., 2019b) that locally introduce immunogenic moieties. Introduction thereof could then help activate the immune system and promote clearance of the infectious agent. Another potential application of the presented concept is in the field of vaccinology. Despite the challenging regulatory complexity of bringing live attenuated vaccines to the clinic, there nevertheless exist several – most notably, against tuberculosis and malaria – that continue to be the subject of active investigation (Pai et al., 2016; Roestenberg et al., 2009; Seder et al., 2013). As these vaccines are still characterized by suboptimal performance attributed to a low immunogenicity (Behr and Small, 1997; Jongo et al., 2021), chemical modification could help provide a much needed boost in immunogenicity.

Conclusion

In conclusion, we have here shown that supramolecular introduction of a TLR7 agonist-based adjuvant (CL307) onto poorly immunogenic *S. aureus* bacteria yields increased production of the key pro-inflammatory cytokine IL-6. Future work will need to determine whether a similarly improved immune response is more broadly observed for other players of the immune system in the context of antimicrobial responses, such as neutrophils, and whether such improvements

ultimately help the immune system more effectively clear poorly immunogenic pathogens. A key area of research to this end will be investigating how the presented concept translates to an in vivo setting. Eventually, positive findings could open up the possibility of using chemical functionalization of (microbial) cells to fine-tune immunological properties, and in this way rationally guide effective immune responses.

References

Ballou, E.R., Avelar, G.M., Childers, D.S., Mackie, J., Bain, J.M., Wagener, J., Kastora, S.L., Panea, M.D., Hardison, S.E., Walker, L.A., *et al.* (2016). Lactate signalling regulates fungal beta-glucan masking and immune evasion. Nat Microbiol *2*, 16238.

Behr, M.A., and Small, P.M. (1997). Has BCG attenuated to impotence? Nature *389*, 133-134.

Buvari, A., and Barcza, L. (1979). Beta-Cyclodextrin Complexes of Different Type with Inorganic-Compounds. Inorg Chim Acta *33*, L179-L180.

Cadoz, M. (1998). Potential and limitations of polysaccharide vaccines in infancy. Vaccine *16*, 1391-1395.

Cambier, C.J., Takaki, K.K., Larson, R.P., Hernandez, R.E., Tobin, D.M., Urdahl, K.B., Cosma, C.L., and Ramakrishnan, L. (2014). Mycobacteria manipulate macrophage recruitment through coordinated use of membrane lipids. Nature *505*, 218-222.

Chen, H., Liu, C., Chen, D., Madrid, K., Peng, S., Dong, X., Zhang, M., and Gu, Y. (2015). Bacteria-Targeting Conjugates Based on Antimicrobial Peptide for Bacteria Diagnosis and Therapy. Mol Pharm *12*, 2505-2516.

Chen, X., and Alonzo, F., 3rd (2019). Bacterial lipolysis of immune-activating ligands promotes evasion of innate defenses. Proc Natl Acad Sci U S A *116*, 3764-3773.

Di Pasquale, A., Preiss, S., Da Silva, F.T., and Garcon, N. (2015). Vaccine Adjuvants: from 1920 to 2015 and Beyond. Vaccines *3*, 320-343.

Duszenko, N., van Willigen, D., M, Welling, M.M., de Korne, C.M., van Schuijlenburg, R., Winkel, B., M.F, van Leeuwen, F.W.B., and Roestenberg, M. (2020a). A supramolecular platform technology for bacterial cell surface modification. ACS Inf Dis *6*, 1734-1744.

Duszenko, N., van Willigen, D.M., Welling, M.M., de Korne, C.M., van Schuijlenburg, R., Winkel, B.M.F., van Leeuwen, F.W.B., and Roestenberg, M. (2020b). A Supramolecular Platform Technology for Bacterial Cell Surface

Modification. ACS Infect Dis *6*, 1734-1744.

Ebenhan, T., Zeevaart, J.R., Venter, J.D., Govender, T., Kruger, G.H., Jarvis, N.V., and Sathekge, M.M. (2014). Preclinical evaluation of 68Ga-labeled 1,4,7-triazacyclononane-1,4,7-triacetic acid-ubiquicidin as a radioligand for PET infection imaging. J Nucl Med *55*, 308-314.

Flannagan, R.S., Heit, B., and Heinrichs, D.E. (2015). Antimicrobial Mechanisms of Macrophages and the Immune Evasion Strategies of Staphylococcus aureus. Pathogens *4*, 826-868.

Francica, J.R., Lynn, G.M., Laga, R., Joyce, M.G., Ruckwardt, T.J., Morabito, K.M., Chen, M., Chaudhuri, R., Zhang, B., Sastry, M.*, et al.* (2016). Thermoresponsive Polymer Nanoparticles Co-deliver RSV F Trimers with a TLR-7/8 Adjuvant. Bioconjug Chem *27*, 2372-2385.

Gault, J., Ferber, M., Machata, S., Imhaus, A.F., Malosse, C., Charles-Orszag, A., Millien, C., Bouvier, G., Bardiaux, B., Pehau-Arnaudet, G.*, et al.* (2015). Neisseria meningitidis Type IV Pili Composed of Sequence Invariable Pilins Are Masked by Multisite Glycosylation. PLoS Pathog *11*, e1005162.

Hensbergen, A.W., Buckle, T., van Willigen, D.M., Schottelius, M., Welling, M.M., van der Wijk, F.A., Maurer, T., van der Poel, H.G., van der Pluijm, G., van Weerden, W.M.*, et al.* (2020). Hybrid Tracers Based on Cyanine Backbones Targeting Prostate-Specific Membrane Antigen: Tuning Pharmacokinetic Properties and Exploring Dye-Protein Interaction. J Nucl Med *61*, 234-241.

Huang, N., Chen, X., Zhu, X., Xu, M., and Liu, J. (2017). Ruthenium complexes/polypeptide self-assembled nanoparticles for identification of bacterial infection and targeted antibacterial research. Biomaterials *141*, 296-313.

Jongo, S.A., Urbano, V., Church, L.W.P., Olotu, A., Manock, S.R., Schindler, T., Mtoro, A., Kc, N., Hamad, A., Nyakarungu, E.*, et al.* (2021). Immunogenicity and Protective Efficacy of Radiation-Attenuated and Chemo-Attenuated Pf-SPZ Vaccines in Equatoguinean Adults. Am J Trop Med Hyg *104*, 283-293.

Medzhitov, R. (2007). Recognition of microorganisms and activation of the immune response. Nature *449*, 819-826.

Mochida, K., Kagita, A., Matsui, Y., and Date, Y. (1973). Effects of Inorganic

Salts on Dissociation of a Complex of Beta-Cyclodextrin with an Azo Dye in an Aqueous-Solution. B Chem Soc Jpn *46*, 3703-3707.

Pai, M., Behr, M.A., Dowdy, D., Dheda, K., Divangahi, M., Boehme, C.C., Ginsberg, A., Swaminathan, S., Spigelman, M., Getahun, H.*, et al.* (2016). Tuberculosis. Nat Rev Dis Primers *2*, 16076.

Pidwill, G.R., Gibson, J.F., Cole, J., Renshaw, S.A., and Foster, S.J. (2020). The Role of Macrophages in Staphylococcus aureus Infection. Front Immunol *11*, 620339.

Roestenberg, M., McCall, M., Hopman, J., Wiersma, J., Luty, A.J., van Gemert, G.J., van de Vegte-Bolmer, M., van Schaijk, B., Teelen, K., Arens, T.*, et al.* (2009). Protection against a malaria challenge by sporozoite inoculation. N Engl J Med *361*, 468-477.

Rood, M.T., Spa, S.J., Welling, M.M., Ten Hove, J.B., van Willigen, D.M., Buckle, T., Velders, A.H., and van Leeuwen, F.W. (2017). Obtaining control of cell surface functionalizations via Pre-targeting and Supramolecular host guest interactions. Sci Rep *7*, 39908.

Rutgers, T., Gordon, D., Gathoye, A.M., Hollingdale, M., Hockmeyer, W., Rosenberg, M., and Dewilde, M. (1988). Hepatitis-B Surface-Antigen as Carrier Matrix for the Repetitive Epitope of the Circumsporozoite Protein of Plasmodium-Falciparum. Bio-Technol *6*, 1065-1070.

Seder, R.A., Chang, L.J., Enama, M.E., Zephir, K.L., Sarwar, U.N., Gordon, I.J., Holman, L.A., James, E.R., Billingsley, P.F., Gunasekera, A.*, et al.* (2013). Protection against malaria by intravenous immunization with a nonreplicating sporozoite vaccine. Science *341*, 1359-1365.

Sica, A., Erreni, M., Allavena, P., and Porta, C. (2015). Macrophage polarization in pathology. Cell Mol Life Sci *72*, 4111-4126.

Spa, S.J., Welling, M.M., van Oosterom, M.N., Rietbergen, D.D.D., Burgmans, M.C., Verboom, W., Huskens, J., Buckle, T., and van Leeuwen, F.W.B. (2018). A Supramolecular Approach for Liver Radioembolization. Theranostics *8*, 2377-2386.

Welling, M.M., de Korne, C.M., Spa, S.J., van Willigen, D.M., Hensbergen,

A.W., Bunschoten, A., Duszenko, N., Smits, W.K., Roestenberg, M., and van Leeuwen, F.W.B. (2019a). Multimodal Tracking of Controlled Staphylococcus aureus Infections in Mice. ACS Infect Dis *5*, 1160-1168.

Welling, M.M., Duszenko, N., van Willigen, D.M., Smits, W.K., Buckle, T., Roestenberg, M., and van Leeuwen, F.W.B. (2021). Cyclodextrin/Adamantane-Mediated Targeting of Inoculated Bacteria in Mice. Bioconjug Chem *32*, 607-614.

Welling, M.M., Paulusma-Annema, A., Balter, H.S., Pauwels, E.K., and Nibbering, P.H. (2000). Technetium-99m labelled antimicrobial peptides discriminate between bacterial infections and sterile inflammations. Eur J Nucl Med *27*, 292-301.

Welling, M.M., Spa, S.J., van Willigen, D.M., Rietbergen, D.D.D., Roestenberg, M., Buckle, T., and van Leeuwen, F.W.B. (2019b). In vivo stability of supramolecular host-guest complexes monitored by dual-isotope multiplexing in a pre-targeting model of experimental liver radioembolization. J Control Release *293*, 126-134.

Wilson, J.T., Keller, S., Manganiello, M.J., Cheng, C., Lee, C.C., Opara, C., Convertine, A., and Stayton, P.S. (2013). pH-Responsive nanoparticle vaccines for dual-delivery of antigens and immunostimulatory oligonucleotides. ACS Nano *7*, 3912-3925.

Zavadovskaya, V.D., Larkina, M.S., Stasyuk, E.S., Zorkaltsev, M.A., Udodov, V.D., Ivanov, V.V., Shevtsova, N.M., Rogov, A.S., Lushchyk, A.Y., Yantsevich, A.V.*, et al.* (2021). Radiolabeled Complex of Antimicrobial Peptides UBI29-41 and UBI18-35 Labeled with (99m)Tc for Differential Diagnosis of Bone Infection of the Limbs. Bull Exp Biol Med *170*, 415-419.

Methods

Full procedures related to synthesis and analysis of the chemical compounds used can be found in the Supplemental Information.

Synthesis of supramolecular components

To create the Ad-UBI_{29-41} compound for pre-functionalizing the bacterial cell surface with supramolecular guest, a UBI29-41 peptide (H-TGRAKRRMQYN-RR-NH2) was synthesized in-house by automated Fmoc-based SPPS. Subsequently, Fmoc-Lys(Fmoc)-OH was coupled manually to the liberated N-terminus of the resin-bound peptide using PyBOP and DiPEA in DMF. After Fmoc deprotection of the lysine sidechain and N-terminus, Fmoc-Gly-OH was coupled using PyBOP and DiPEA by agitating in DMF. The glycine amines were liberated and, finally, 1-adamantanecarbonyl chloride was coupled using 1-hydroxybenzotriazole and DiPEA by agitating in DMF. The peptide was then cleaved by adding a mixture of v/v 38:1:1 TFA:TIPS:H2O and agitating for 3 hours, whereafter the mixture was added to ice-cold MTBE:Hexane 1:1. The crude peptide was collected by centrifugation, whereafter the pellet was resuspended in ice-cold MTBE:Hexane twice, followed by drying in vacuo. The off-white solid was then purified using preparative HPLC, followed by lyophilization to yield the white solid product.

To create the adjuvant-bearing host polymer $CD_{85}Cy5_2CL307_{58}$PIBMA for complexing onto Ad-pre-functionalized bacterial cell surface, poly(isobutylene-alt-maleic-anhydride was dissolved in dimethylsulfoxide, whereafter amino(6-monodeoxy-6-mono)-β-cyclodextrin hydrochloride and N,N-Diisopropylethylamine were added, followed by stirring at 80°C for 94 hours. The solution was purified by dialysis in water for 7 hours, followed by dialysis in phosphate buffer (0.2 M, pH 9) for 144 hours including refreshment of buffer twice, followed by dialysis in water for 7 hours. The dialysate was discarded and the residue was lyophilized, yielding an off-white solid. The product $PIBMA_{[389]}$-$CD_{[85]}$ was subsequently dissolved in water, whereafter N,N'-diisopropylcarbodiimide was added. The mixture was stirred at room temperature for 1 hour followed by addition of NH2-Cy5-COOH. The solution was stirred for 5 hours at room temperature whereafter it was dialysed in water for 24 hours with one refresh of water, followed by lyophilization of the product. The product $PIBMA_{[389]}$-$CD_{[85]}$-$Cy5_{[2]}$ was dissolved in water, followed by addition of DIC. After stirring for 1.3 hours at room temperature, CL307 was added. After shaking for 1.3 hours, ethanolamine was added and stirring was continued for another 16 hours at room temperature. Thereafter, the reaction mixture was dialyzed in water for 29 hours with one refreshment of water. The resulting adjuvant-bearing host polymer $CD_{85}Cy5_2CL307_{58}$PIBMA was used as is for experiments; PBS pH 7.4

was added where necessary.

Supramolecular complexation of CL307-bearing polymers onto S. aureus cell surface

S. aureus stocks (strain ATCC 29213) were thawed from -20 °C and washed twice in 25 mM ammonium acetate buffer pH 5 by centrifugation at 10k RCF for 5 minutes and subsequent removal of supernatant by pipet. From this washed stock, 108 bacteria were added to 1 mL of an 8 μM solution of Ad-UBI_{29-41} in 25 mM ammonium acetate buffer pH 5 and incubated for 30 minutes at 37 °C with shaking. Thereafter, bacteria were thrice washed with PBS containing 1% albumin by centrifugation at 10k RCF for 5 minutes and subsequent removal of supernatant by decanting. Washed, Ad-pre-functionalized bacteria were re-suspended in 1 mL PBS, wherefrom 100 μL aliquots were added to 100 μL of a 2 μM solution of the adjuvant-bearing host polymer ($CD_{85}Cy5_2CL307_{58}$PIB-MA) in PBS at a concentration of 1.9X (where 1X is equivalent to standard commercial PBS) and incubated overnight at 37 °C with shaking. Thereafter, bacteria were thrice washed with PBS containing 1% albumin by centrifugation at 10k RCF for 5 minutes and subsequent removal of supernatant by decanting. Washed, adjuvanted bacteria were then resuspended in PBS or RPMI for down-stream applications.

Analysis of adjuvanted S. aureus

To visually confirm the presence of CL307-bearing host polymers on the S. aureus surface via the polymers' Cy5 reporter, 10 μL aliquots (with the addition of 10 μg/mL Hoechst 33342) of adjuvanted bacteria were added to glass-bottom confocal dishes (MatTek Corporation, Ashland, MA, USA), overlaid with a coverslip and analyzed with a Leica (Wetzlar, Germany) SP8 confocal fluorescence microscope; Hoechst signal was acquired using a 405 nm laser at 20% maximal output and a HyD detector set to 425-475 nm, Cy5 signal was acquired using a 633 nm laser at 5% maximal output and a HyD detector set to 650-700 nm. Post-acquisition analyses of microscopic images was performed using Leica LasX and ImageJ software.

To quantitatively assay the presence of CL307-bearing host polymers on the S. aureus surface, adjuvanted bacteria were run through a BD (Franklin Lakes, NJ, USA) FACSCanto II instrument using signal acquisition in the instrument's "APC" channel to provide a quantitative measure of CL307-bearing host polymers present on the bacterial surface. Alongside adjuvanted bacteria, commercial fluorescence quantification beads (Bangs Laboratories, Inc., Fishers, IN, USA) were run on the instrument to generate a standard curve for converting the instrument's fluorescent signal intensities of arbitrary values to absolute values. Post-acquisition analyses was performed with FlowJo 10 software (Ashland, OR, USA).

For assessing stability of CL307-polymers complexed to the S. aureus surface, adjuvanted bacteria were incubated at 37 °C in PBS for up to 24 hours. For assessing their growth, bacteria were incubated at 37 °C in brain heart infusion growth media with shaking for 16 hours.

Immune response to adjuvanted S. aureus

Monocyte-derived macrophages were prepared as previously described.[16] To visually confirm that adjuvanted S. aureus could still be phagocytosed by macrophages, harvested macrophages were plated at a density of 100k macrophages in 200 μL RPMI containing 10% FBS onto glass-bottom confocal dishes and incubated overnight at 37 °C. The next day, 1.8 mL RPMI 10% FBS containing 10 μg/mL Hoechst 33342 was added to the confocal dishes and the dishes positioned on an Andor (Belfast, Northern Ireland) Dragonfly 500 spinning disk confocal fluorescence microscope. Immediately before image acquisition, a 10 μL aliquot containing 106 adjuvanted bacteria was carefully added just above the macrophage layer. Subsequently, z-stack images of approximately 40 μm in depth at 1 μm intervals were acquired every 2.5 minutes for a total duration of 30 minutes. Post-acquisition analyses of images were performed using Imaris software (Zurich, Switzerland).

To assay the immunogenicity of adjuvanted S. aureus, macrophages post-harvesting were plated at a density of 100k macrophages in 100 μL RPMI 10% FBS in 96-well flat-bottom plates (Nunc, Thermo Fisher Scientific, Waltham, MA, USA) and incubated overnight at 37 °C. The next day, 400k adjuvanted bacteria in 100 μL RPMI 10% FBS were added to the wells, and the macrophages incubated for another 24 hours. Following this, supernatants were removed from wells and stored at -20 °C for eventual cytokine analysis using BD Biosciences human IL-6 (Cat. No. 555220) and IL-10 (Cat. No. 555157) ELISA kits according to the manufacturer's specifications.

Statistical analyses

Significance of differences between groups was analyzed by ANOVA with t-test for multiple comparison's or Student's t-test for two groups, using Graphpad Prism 9.3.1.

Supplementary Information

Chemical Procedures

1. General

1.1 Chemicals

Chemicals were obtained commercially from Merck (Darmstadt, Germany), TCI (Tokyo, Japan) or Cyclodextrin-Shop (Tilburg, The Netherlands) and used without further purification; these were deemed free of any significant endotoxin contamination by respective manufacturers. Amino acids were obtained from either Bachem (Bubendorf, Switzerland) or Iris Biotech (Marktredwitz, Germany). Solvents were obtained from Actu-All (Oss, The Netherlands), Biosolve (Valkenswaard, The Netherlands) or Merck (Darmstadt, Germany). Acetonitrile, N,N-Dimethylformamide and Dimethylsulfoxide were dried using 4Å molecular sieves Merck (Darmstadt, Germany) unless stated otherwise. Reactions were carried out under normal atmosphere unless stated otherwise. Column chromatography was performed with 40–63 μm silica from Screening Devices (Amersfoort, The Netherlands). SPPS was carried out either by a Biotage Syro II (Uppsala, Sweden) or by hand using fritted tubes (6, 10 or 25 mL) from Screening Devices (Amersfoort, The Netherlands) and in-house N_2 flow/vacuum.

1.2 HPLC

High-performance liquid chromatography was performed on a Waters HPLC system using either a 1525EF or 2545 pump and a 2489 UV/VIS detector. For preparative HPLC either a Dr. Maisch GmbH Reprosil-Pur 120 C18-AQ 10 *μm* (250 × 20 mm) column using a flow of 12 mL/min or an XBridge Prep C8 10 *μm* OBD (250 × 30 mm column) with a flow of 25 mL/min was used. For semi-preparative HPLC a Dr. Maisch GmbH Reprosil-Pur C18-AQ 10 *μm* (250 × 10 mm) column was used with a flow of 5 mL/min. For analytical HPLC a Dr. Maisch GmbH Reprosil-Pur C18-AQ 5 *μm* (250 × 4.6 mm) column with a flow of 1 mL/min and a gradient of 5→95% CH_3CN in H_2O) (0.1% TFA) in 40 min (1 mL/min) was used.

1.3 Mass spectrometry

Mass spectrometry was performed using a Bruker Microflex Matrix-assisted laser desorption ionization time-of-flight (MALDI-TOF) mass spectrometer (Billerica, MA, United States).

1.4 NMR

^{1}H NMR, COSY and ^{13}C NMR of the dyes were recorded on a Bruker AV-300 spectrometer (300 MHz) (Billerica, MA, United States) in methanol-d_4. Quantification of the number of β-CD units per polymer with ^{1}H NMR and DOSY was done in D_2O using a Bruker Avance III spectrometer (500 MHz), equipped with a 5 mm TXI probe.

1.5 Dialysis

Dialysis was performed using Pur-A-Lyzer (either Mega/Maxi 3500 MWCO or Mini 12000 MWCO) dialysis kits from (Sigma-Aldrich, St. Louis, MO, USA).

1.6 Photometry

Absorbance spectra were recorded using an Ultrospec 2100 pro (Amersham Biosciences, Little Chalfont, United Kingdom).

2. Chemical analyses

2.1 Quantification of β-CD

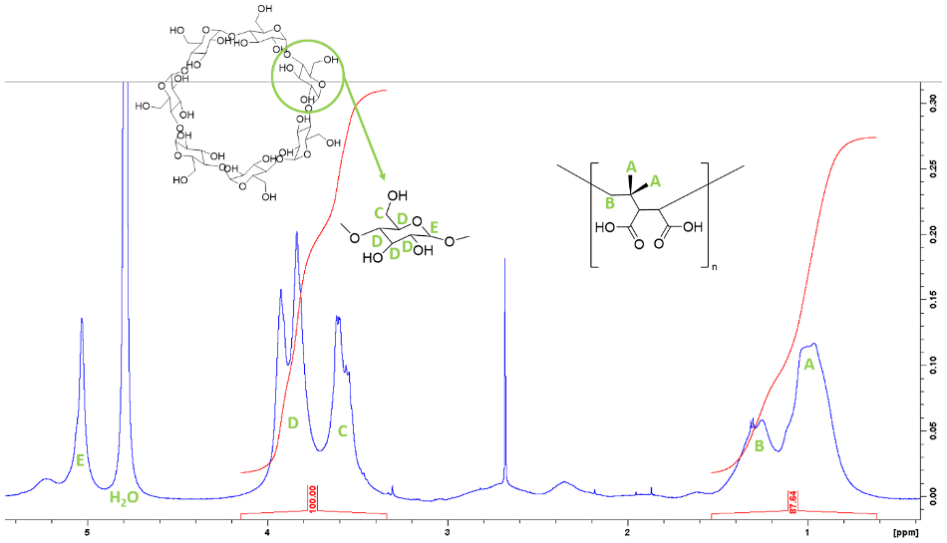

Figure S1: ^{1}H NMR spectrum with integrated peaks and annotation of *PIB-MA$_{[389]}$-CD$_{[85]}$ (6)* confirming presence of β-CD, which was used for calculation of the average amount of β-CD per polymer unit.

The amount of β-CD per polymer was determined as previously described (Duszenko et al., 2020b; Rood et al., 2017) using ^{1}H NMR; briefly: the polymer peaks at 0.8 - 1.4 ppm (CH_3 and CH_2) were integrated (87.6), as well as the β-CD peaks at 4.0 - 3.5 ppm originating from the β-CD protons. These integrals were used for calculation of the amount of β-CD per polymer using the following rationale:

Monomer protons=βCD protons=87.6 : 100=8 : 9.13

βCD per monomer=(Integrated βCD protons)/(Total protons in βCD)= 9.13/42=0.217 βCD=1 βCD per 4.6 monomers

βCD units per polymer unit=(Monomer units per polymer)/(Monomer units per βCD)= 389/4.6=84.6

This was rounded to 85 for clarity of illustration and calculation.

2.2 Quantification of Cy5

The molar extinction coefficient of NH_2-Cy5-COOH was determined as previously described;(Hensbergen et al., 2020) briefly: a weighed amount of Cy5 was dissolved in water to create a 5 mM stock solution. From this stock a dilution range from 7.5 μm to 0.25 μm was made in triplicate, of which the absorption was measured at Abs_{max} = 640 nm. Using linear regression, the molar extinction coefficient was then determined to be 62900 $L^{-1} \cdot mol^{-1} \cdot cm^{-1}$ in water. This was used with the Lambert-Beer equation to determine the dye molarity in a 3.1 μM solution of **$PIBMA_{[389]}$-$CD_{[85]}$-$Cy5_{[x]}$ (7)**. Dividing the dye molarity by 3.1 μM thus provided an average number of 1.53 Cy5 molecules per polymer; for clarity of illustration and calculation this was rounded to 2 Cy5 dyes per polymer.

2.3 Quantification of CL307 (the adjuvant) on polymer

The molar extinction coefficient of CL307 was estimated as previously described (Hensbergen et al., 2020); briefly: a weighed quantity of CL307 was dissolved in water to yield a 1 mM stock solution. From this stock a dilution range from 7.5 μm to 0.25 μm was made in triplicate, of which the absorption was measured at Abs_{max} = 298 nm. Using linear regression, the molar extinction coefficient was determined to be 5200 $L^{-1} \cdot mol^{-1} \cdot cm^{-1}$ in water. This was used with the Lambert-Beer equation to determine the CL307 molarity in a 0.5 μM solution of **$PIBMA_{[389]}$-$CD_{[85]}$-$Cy5_{[2]}$-$CL307_{[x]}$ (9)**. Dividing the CL307 molarity by 0.5 μM thus gave an average number of 58 CL307 molecules per polymer.

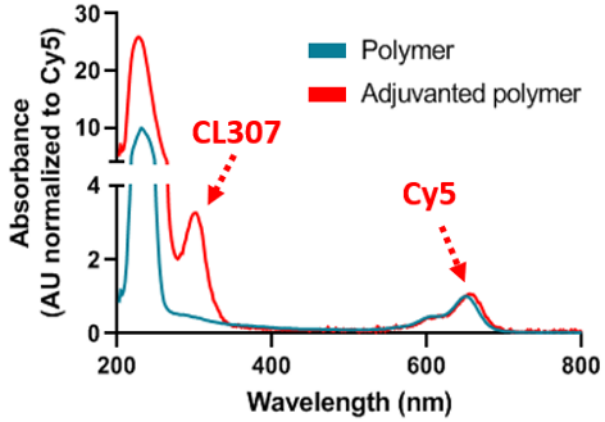

Figure S2: Confirmation of CL307 presence on the polymer was obtained using UV-Vis spectroscopy by measuring a solution of $PIBMA_{[389]}$-$CD_{[85]}$-$Cy5_{[2]}$-$CL307_{[58]}$-$NEtOH_{[633]}$ (9) in water (red line). This shows amide-bond absorption around 214 nm, absorption of CL307 around 300 nm and Cy5 absorption around 650 nm. As a control, $PIBMA_{[389]}$-$CD_{[85]}$-$Cy5_{[2]}$ (7) was also measured (turquoise line) showing only amide-bond and Cy5 absorption around 214 nm and 650 nm, respectively.

2.4 HPLC

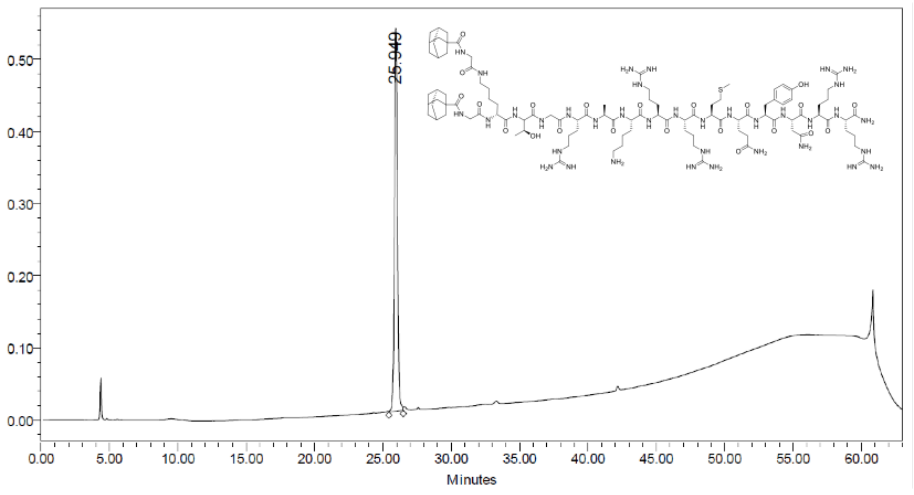

Figure S3: HPLC (220 nm) of *UBI-Lys(Gly-Ad)$_2$ (1.)*

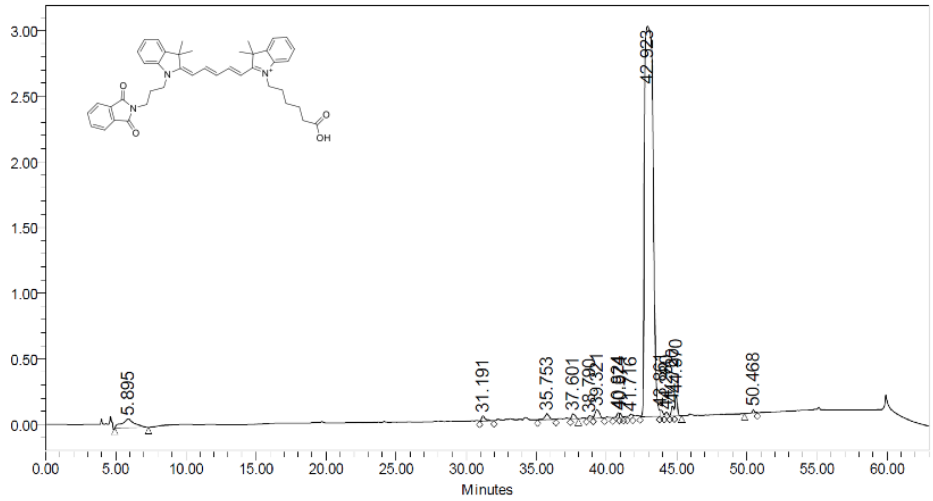

Figure S4: HPLC (220 nm) of Phth-Cy5-COOH (4).

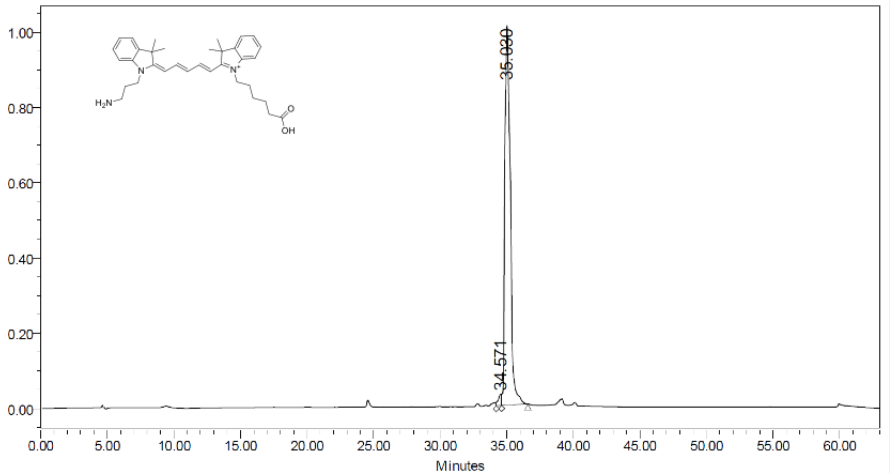

Figure S5: HPLC (220 nm) of NH_2-Cy5-COOH (5).

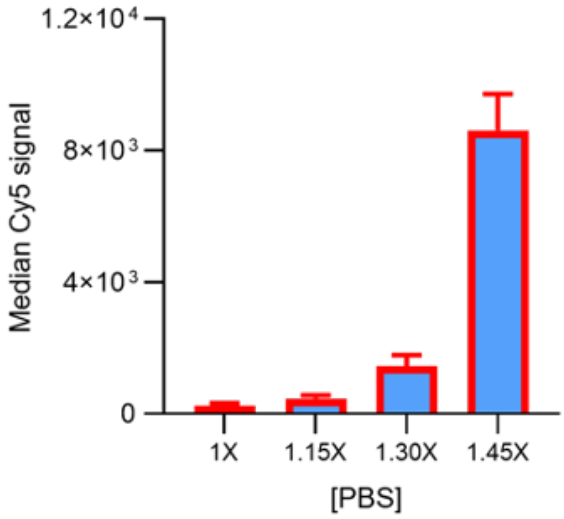

Figure S6: Complexation of adjuvant-bearing polymers onto *S. aureus* at varying PBS concentrations. Median Cy5 signal (y-axis) of complexed adjuvant-bearing polymer at differing concentrations of PBS (x-axis) during complexation.

Supplementary References

[1] D. Oushiki, H. Kojima, T. Terai, M. Arita, K. Hanaoka, Y. Urano, T. Nagano, *J Am Chem Soc* **2010**, *132*, 2795-2801.

[2] A. W. Hensbergen, T. Buckle, D. M. van Willigen, M. Schottelius, M. M. Welling, F. A. van der Wijk, T. Maurer, H. G. van der Poel, G. van der Pluijm, W. M. van Weerden, H. J. Wester, F. W. B. van Leeuwen, *J Nucl Med* **2020**, *61*, 234-241.

[3] M. T. Rood, S. J. Spa, M. M. Welling, J. B. Ten Hove, D. M. van Willigen, T. Buckle, A. H. Velders, F. W. van Leeuwen, *Sci Rep* **2017**, *7*, 39908.

[4] N. Fattahi, M. Ayubi, A. Ramazani, *Tetrahedron* **2018**, *74*, 4351-4356.

[5] N. Duszenko, D. M. van Willigen, M. M. Welling, C. M. de Korne, R. van Schuijlenburg, B. M. F. Winkel, F. W. B. van Leeuwen, M. Roestenberg, *ACS Infect Dis* **2020**, *6*, 1734-1744.